EXPLORATION OF THE MARS POLAR ATMOSPHERE USING MCS AND EMARS

H. E. Gillespie[1], S. J. Greybush[1], D. J. McCleese[2], A. Kleinböhl[3], D. M. Kass[3], R. J. Wilson[4] and J. T. Schofield[3]

[1]Penn State, University Park, PA (hjg5116@psu.edu), [2]Synoptic Science, Altadena, CA, [3]Jet Propulsion Laboratory, California Institute of Technology, Pasadena, CA, [4]Ames Research Center, Mountain View, CA

Introduction:

Observations of the Martian atmosphere obtained from the Mars Climate Sounder (MCS) are compared with Ensemble Mars Atmosphere Reanalysis System (EMARS) simulations and applied to the study of the polar atmosphere. The polar atmosphere has been the subject of a wide variety of investigations, e.g. [1]. The crucial features of the polar vortices include sharp temperature and wind gradients throughout the depth of the atmosphere, transient and stationary wave activity, tides, deposition of CO_2, and the presence of water ice and dust aerosols.

Data and Methods:

MCS is an instrument aboard the polar-orbiting Mars Reconnaissance Orbiter spacecraft that provides vertical profiles of temperature, dust opacity, and water ice at approximately 3 AM and 3 PM; additional local times are measured using cross-track observations [2]. MCS follows in the footsteps of and improves on the Thermal Emission Spectrometer (TES) dataset [3]. Both the vertical range and resolution of MCS are doubled compared to TES [2]. Recent 2-D retrievals improve the quality of MCS observations in regions with sharp temperature gradients, which are especially relevant in the study of the polar vortex [4].

EMARS is a Mars reanalysis that combines information from a Martian climate model and observations of the Martian atmosphere to estimate the state of the Martian atmosphere [5]. EMARS combines the Geophysical Fluid Dynamics Laboratory Mars General Circulation Model (GFDL MGCM) [6] and MCS observations using the local ensemble transform Kalman filter (LETKF) [7]. MCS temperature observations are assimilated, and temperature, wind, and surface pressure are updated by the LETKF based on the covariances of the ensemble members. Dust is advected in the model and adjusted in the boundary layer to correspond to the Montabone [8] dust product. We also compare to a freely running simulation by the MGCM, using the same dust as EMARS.

Results:

Figures 1 and 2 show zonal and time mean cross-sections at constant local time over the northern pole. Figure 1 shows MCS observations, while Figure 2 shows the EMARS reanalysis at 3 AM and 3 PM, which are typical MCS observation local times. There are several similarities between the MCS observations and the EMARS reanalysis. The zonal mean temperature structure is qualitatively similar. The polar front is located at about 65 N at 100 Pa, and the core of the polar vortex has a minimum temperature of about 125 K at 10 Pa. Figure 3 shows additional EMARS fields; the maxima in zonal wind are another indicator of the location of the polar vortex, which follows the sharp temperature gradients. Dust is concentrated in the tropics in both MCS and EMARS. Both also show ice clouds between 10 and 30 Pa over the tropics.

Several differences between MCS and EMARS are immediately apparent, and these differences suggest potential research topics of interest, including the thermal tides, aerosol distribution and transport, and CO_2 latent heating.

Thermal Tides: In the temperature plots, the diurnal tide (AM / PM differences) below 300 Pa has a larger amplitude in MCS than in EMARS. There are cold regions in MCS between 40 and 60 N at a height of approximately 2 Pa, and regions of high ice mixing ratio lie below these cold regions; we conjecture that these are signatures of a semidiurnal tide not represented as strongly in EMARS. We also have compared the tidal amplitudes and phases in both EMARS and the MGCM (not shown).

Aerosols and Transport: A detached dust layer is evident over the equator in both the morning and afternoon in MCS and not present in this version of EMARS; the presence of these features would require the application of more sophisticated dust assimilation techniques [9]. Transport of dust into the vortex is another topic of exploration.

Water ice in the MCS polar vortex is mostly above 100 Pa, while EMARS water ice is below that pressure level. The plot of EMARS water vapor (Fig. 3) shows a depletion of water vapor in and above the equatorial ice cloud region and within the core of the vortex. EMARS relative humidity plots (not shown) show that the interior of the vortex and the equatorial ice clouds are saturated with vapor and that the boundary of the vortex is demarcated by a transition between a saturated and unsaturated atmosphere.

CO_2 Latent Heating: There is a “dusty” region in Figure 1 at about 10 Pa over the winter pole; this is suggestive of deposition of CO_2 at that altitude because the radiative properties of solid CO_2 particles are similar to those of dust in the infrared bands that MCS observes. The latent heating from CO_2 implied in EMARS over the north pole (Fig. 3) corroborates that the MCS “dust” observation over the pole is actually an observation of CO_2 ice clouds. We have created Hovmöller-like plots (not shown) of latent heating by CO_2 deposition in the MGCM and EMARS

around northern winter solstice on the native model levels approximately 1 km above ground level (AGL), 12 km AGL, and at 24 Pa. In the MGCM, latent heating is evidently influenced by the diurnal tide, stationary waves, and transient eddies. The apparent influence of transient eddies on latent heating in EMARS is decreased with respect to the MGCM, while the influence of the diurnal tide and stationary waves is increased, especially at 12 km AGL. Stationary waves are evident: a minimum of latent heating is evident at 240 E, and a secondary minimum is present at 30 E; maxima are located at 90 E and 340 E.

Acknowledgements: Work at the Jet Propulsion Laboratory, California Institute of Technology is performed under contract with NASA. Funded by NASA grants NNX11AL25G, NNX14AM13G and 80NSSC17K0690.

References:

[1] Waugh, D. W. et al. (2016), *J. Geophys. Res. Planets*, *121*, 1770-1785. [2] McCleese, D. J. et al. (2007), *J. Geophys. Res.*, *112*, E05S06. [3] Smith, M. D. et al. (2001), *J. Geophys. Res.*, *106*, E10, 23929-23945. [4] Kleinböhl, A. et al. (2017), *JQSRT*, *187*, 511-522. [5] Greybush, S. J. et al. (2014), Ensemble Mars atmosphere reanalysis system (EMARS), *Presented at the 5th MAMO International Workshop*. [6] Wilson, R. J. et al. (2002), *Geophys. Res. Lett.*, *29*, 1684-1687. [7] Hunt, B. R. et al. (2007), *Physica D*, *230*, 112-126 [8] Montabone, L. et al. (2015), *Icarus*, *251*, 65-95. [9] Navarro, T. et al. (2017), *Earth and Space Science*, *4*, 690–722.

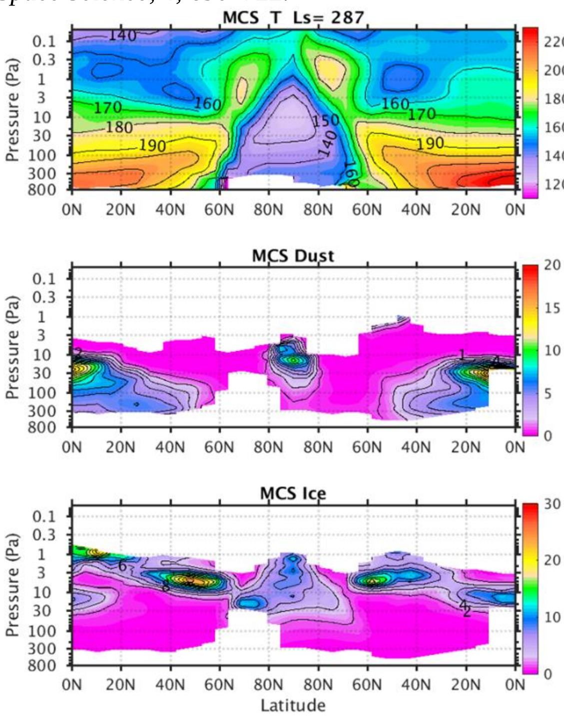

Figure 1: MCS temperature (K, top), dust mass mixing ratio (ppm, middle) and ice mass mixing ratio (ppm, bottom) in MY 30, Ls 287. Morning temperatures are shown on the left half of the plots, while afternoon temperatures are on the right half. Quantities are averaged over 5 Ls, centered on Ls 287.5.

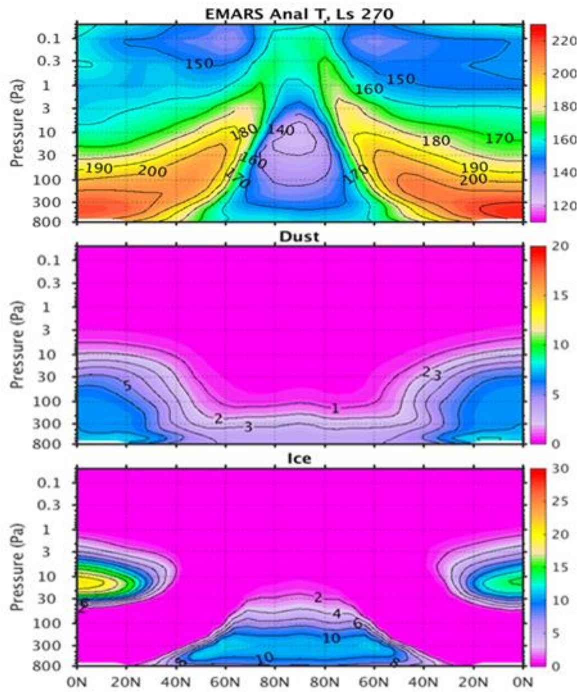

Figure 2: EMARS temperature (K, top), dust mass mixing ratio (ppm, middle) and ice mass mixing ratio (ppm, bottom) in MY 30, Ls 270. 3 AM temperatures are shown on the left half of the plots, while 3 PM temperatures are on the right half. Quantities are averaged over 20 sols.

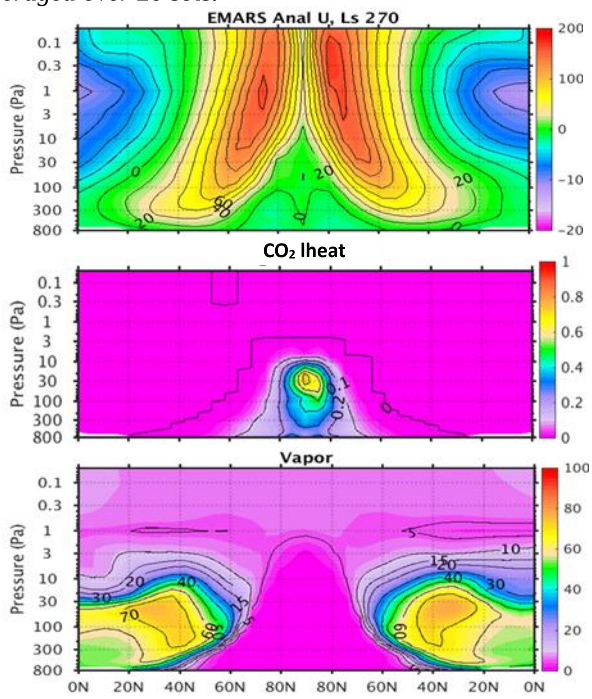

Figure 3: EMARS zonal wind (m/s, top), CO_2 latent heating (K/hr, middle), and water vapor mass mixing ratio (ppm, bottom) in MY 30, Ls 270. Morning temperatures are shown on the left half of the plots, while afternoon temperatures are on the right half. Quantities are averaged over 20 sols.

